



HHS Public Access

Author manuscript

Biol Psychiatry Cogn Neurosci Neuroimaging. Author manuscript; available in PMC 2022 December 01.

Published in final edited form as:

Biol Psychiatry Cogn Neurosci Neuroimaging. 2021 December ; 6(12): 1202–1214. doi:10.1016/j.bpsc.2020.11.014.

Social Cognitive Networks and Social Cognitive Performance Across Individuals With Schizophrenia Spectrum Disorders and Healthy Control Participants

Lindsay D. Oliver,

Colin Hawco,

Philipp Homan,

Junghee Lee,

Michael F. Green,

James M. Gold,

Pamela DeRosse,

Miklos Argyelan,

Anil K. Malhotra,

Robert W. Buchanan,

Aristotle N. Voineskos,

SPINS Group

Campbell Family Mental Health Research Institute (LDO, CH, ANV), Centre for Addiction and Mental Health, Toronto, and Department of Psychiatry (CH, ANV), University of Toronto, Toronto, Ontario, Canada; University Hospital of Psychiatry (PH), University of Zurich, Zurich, Switzerland; Division of Psychiatry Research (PH, PD, MA, AKM), Zucker Hillside Hospital, Division of Northwell Health, Glen Oaks; Department of Psychiatry (PH, PD, MA, AKM), The Donald and Barbara Zucker School of Medicine at Hofstra/Northwell, Hempstead; and Center for Psychiatric Neuroscience (PH, PD, MA, AKM), Feinstein Institute for Medical Research, Manhasset, New York; Department of Psychiatry and Biobehavioral Sciences (JL, MFG), Semel Institute for Neuroscience and Human Behavior, University of California, Los Angeles, and Department of Veterans Affairs (JL, MFG), Desert Pacific Mental Illness Research, Education, and Clinical Center, Los Angeles, California; Department of Psychiatry and Behavioral Neurobiology (JL), School of Medicine, University of Alabama at Birmingham, Birmingham, Alabama; and Maryland Psychiatric Research Center (JMG, RWB), Department of Psychiatry, University of Maryland School of Medicine, Baltimore, Maryland.

Abstract

BACKGROUND: Schizophrenia spectrum disorders (SSDs) feature social cognitive deficits, although their neural basis remains unclear. Social cognitive performance may relate to neural circuit activation patterns more than to diagnosis, which would have important prognostic and

Address correspondence to Aristotle Voineskos, M.D., Ph.D., at aristotle.voineskos@camh.ca.

The authors report no biomedical financial interests or potential conflicts of interest.

Supplementary material cited in this article is available online at <https://doi.org/10.1016/j.bpsc.2020.11.014>.

therapeutic implications. The current study aimed to determine how functional connectivity within and between social cognitive networks relates to social cognitive performance across individuals with SSDs and healthy control participants.

METHODS: Participants with SSDs ($n = 164$) and healthy control participants ($n = 117$) completed the Empathic Accuracy task during functional magnetic resonance imaging as well as lower-level (e.g., emotion recognition) and higher-level (e.g., theory of mind) social cognitive measures outside the scanner. Functional connectivity during the Empathic Accuracy task was analyzed using background connectivity and graph theory. Data-driven social cognitive networks were identified across participants. Regression analyses were used to examine network connectivity–performance relationships across individuals. Positive and negative within- and between-network connectivity strengths were also compared in poor versus good social cognitive performers and in SSD versus control groups.

RESULTS: Three social cognitive networks were identified: motor resonance, affect sharing, and mentalizing. Regression and group-based analyses demonstrated reduced between-network negative connectivity, or segregation, and greater within- and between-network positive connectivity in worse social cognitive performers. There were no significant effects of diagnostic group on within- or between-network connectivity.

CONCLUSIONS: These findings suggest that the neural circuitry of social cognitive performance may exist dimensionally. Across participants, better social cognitive performance was associated with greater segregation between social cognitive networks, whereas poor versus good performers may compensate via hyperconnectivity within and between social cognitive networks.

Individuals with schizophrenia spectrum disorders (SSDs) often experience persistent debilitating social cognitive deficits (1,2). Such impairments have been associated with poor community functioning and long-term disability (3,4) and have demonstrated stronger relationships with functional outcome than non-social-cognitive deficits (5,6). Social cognition is often divided into lower- and higher-level processes (7–9). Lower-level social cognition includes internal simulation of emotions and actions as well as emotion recognition and simple mental representation. These processes are believed to be subserved by a network including the inferior frontal gyrus, premotor cortex, supplementary motor area, inferior parietal lobule (IPL), and posterior superior temporal sulcus (pSTS) (10–12) as well as regions associated with emotional empathy including the anterior insula and anterior cingulate cortex (ACC) (13–15). Higher-level social cognition involves complex mental state representation (i.e., theory of mind) and is believed to depend on a mentalizing network composed of the medial prefrontal cortex, temporoparietal junction, and posterior cingulate cortex into the precuneus (16,17).

Functional magnetic resonance imaging (fMRI) studies have shown abnormal neural activation in regions of these circuits during social tasks in individuals with SSDs (1,18,19). However, little is known regarding how such regions interact during social cognitive processing. Existing studies of functional connectivity at rest (20–24) and the few studies of functional connectivity during social cognitive processing (25–28) in people with SSDs have yielded inconsistent results, showing hyperconnectivity, hypoconnectivity, and a lack of connectivity differences between social cognitive regions compared to healthy control

participants. Furthermore, there is evidence that neural activation patterns during social processing relate to cognitive performance rather than diagnosis across people with SSDs and healthy control participants (29). In large heterogeneous samples, such as in people with SSDs and other psychiatric disorders, the observed range of behavior and neural circuit activation frequently shows overlap with healthy control participants. This could contribute to inconsistencies in case-control findings, highlighting the importance of examining dimensional brain–behavior relationships across patient and control groups (30–32). Indeed, deficit-specific biological markers might not necessarily be disorder specific (33,34). The inconsistency across studies also raises the question of whether brain network topology supports the division of higher- and lower-level social cognition.

The Empathic Accuracy (EA) task engages a range of social cognitive regions (35–37), making it ideal for investigating the interplay of social cognitive networks. The EA task is a naturalistic social task (35,38,39), aligning with the movement toward narrative naturalistic viewing during fMRI (40,41). It is also amenable to background connectivity analysis, which involves removing the stimulus-evoked response and focusing on residual activation, providing better discrimination of state-related functional connectivity versus stimulus-driven coactivation (42–44).

This paper reports findings from EA task fMRI data from the Social Processes Initiative in the Neurobiology of the Schizophrenia(s) (SPINS), a multicenter Research Domain Criteria study funded by the National Institute of Mental Health. SPINS is a rich multimodal neuroimaging and behavioral investigation designed to capture heterogeneity in social cognition across a large sample of people with SSDs and healthy control participants. Here, we used background connectivity and graph theoretical analyses during the EA task to identify data-driven social cognitive networks and determine how network connectivity relates to social cognitive performance and SSD versus healthy control status. We used regression analyses to examine the continuous relationship between social cognitive network connectivity and social cognitive performance across participants. We also compared within- and between-network connectivity in poor versus good social cognitive performance groups across people with SSDs and healthy control participants and in SSDs versus healthy control groups. We hypothesized that regression analyses would reveal relationships between network connectivity and social cognitive performance across participants with SSDs and healthy control participants. Accordingly, we hypothesized that within- and between-network functional connectivity during the EA task would differ between good and poor social cognitive performers.

METHODS AND MATERIALS

Participants

Participants (164 with SSDs and 117 healthy individuals) were recruited for SPINS from the Centre for Addiction and Mental Health (Toronto, Ontario, Canada), Zucker Hillside Hospital (Glen Oaks, NY), and the Maryland Psychiatric Research Center (Baltimore, MD) from December 2014 to March 2018. Participants with SSDs met DSM-5 criteria for schizophrenia, schizoaffective disorder, schizophreniform disorder, delusional disorder, or psychotic disorder not otherwise specified, assessed using the Structured Clinical

Interview for DSM-IV-TR, and had no change in antipsychotic medication or decrement in functioning/support level during the 30 days prior to enrollment. Additional exclusion criteria included a history of head trauma resulting in unconsciousness, substance use disorder, intellectual disability, debilitating or unstable medical illness, or other neurological diseases (see Supplement for details and inclusion/exclusion criteria for controls). All participants signed an informed consent agreement, and the protocol was approved by the respective research ethics and institutional review boards. All research was conducted in accordance with the Declaration of Helsinki.

Clinical and Cognitive Assessment

Data collection occurred across 3 visits. Out-of-scanner social cognitive measures included the Penn Emotion Recognition Test (45), the Reading the Mind in the Eyes Test (46), and the Awareness of Social Inference Test–Revised (TASIT), parts 1, 2, and 3 (47). Psychiatric symptoms (SSD only), non-social cognition, and social functioning were also assessed (see Supplement).

MRI Data Acquisition

MRI scans were collected using harmonized scanning parameters on five 3T scanners (see Supplement). The EA task was part of a longer multimodal MRI protocol, as previously described (48). Three EA fMRI runs were acquired using an echo-planar imaging sequence (repetition time = 2000 ms, echo time = 30 ms, flip angle = 77°, field of view = 21.8°, in-plane resolution = 3.4 mm², slice thickness = 4 mm). Anatomical T1-weighted scans were collected using a fastgradient sequence (repetition time = 650 ms, echo time = 3 ms, flip angle = 8°, field of view = 23°, in-plane resolution = 0.9 mm², slice thickness = 0.9 mm).

Prior to analysis, all scans were quality checked by experienced research staff using an in-house quality control system dashboard (<https://github.com/TIGRLab/dashboard>), including qualitative monitoring (e.g., detection of ghosting or ringing) and quantitative monitoring (e.g., framewise displacement, signal-to-noise ratio). Individual residual time series and connectivity matrices were also visually examined for abnormalities.

EA Task

The EA task (38,39) was completed during fMRI. In this task, participants watch 9 videos (120–150 seconds each), presented in three runs (~10 min/run), of individuals describing emotional autobiographical events and provide continuous ratings of how positive or negative the individuals in the videos are feeling (see Supplement).

fMRI Preprocessing

All scans were preprocessed using an in-house pipeline system, epitome (<https://github.com/josephdiviviano/epitome>), which uses FSL and AFNI, including slice-time correction, despiking, scaling, linear registration, nonlinear warping, and censoring of time points with framewise displacement >0.5 mm (49). A nuisance regression model was applied to the data, including thorough regression of head motion parameters (50) and tissue-specific regressors (51) but no global signal regression. The data were then smoothed and warped into Montreal Neurological Institute space (see Supplement). An amplitude-modulated general linear

model was performed using AFNI's 3dDeconvolve. For each of the nine EA task videos, one hemodynamic response function was fit for the duration of the video as well as a second hemodynamic response function modulated by the participant's EA score and a third hemodynamic response function modulated by the number of button presses made during the video. These regressors were fit to each voxel to model the stimulus-evoked response, and the residual activation was retained for background connectivity analysis.

Connectivity Matrix Construction

Background connectivity analysis involves removing the modeled stimulus-evoked response and correlating residual activation over time across regions of interest (ROIs). The focus is on state-related rather than stimulus-driven correlations given that stimuli can evoke synchronized activity in multiple brain regions regardless of whether they are interacting (42,43). This is ideal for continuous tasks, and for the EA task in particular, given that we were interested in the state of emotional understanding across videos rather than individual responses to video events.

ROIs were defined using the Shen atlas (52), a whole-brain data-driven parcellation based on resting-state connectivity data that has been used for network analysis (48,53). Cortical ROIs were selected if they included the following canonical and consistently identified areas involved in lower- and higher-level social cognition based on extant meta-analyses and reviews of the literature: the medial prefrontal cortex, temporoparietal junction, pSTS, precuneus, posterior cingulate, anterior insula, ACC, supplementary motor area, inferior frontal gyrus, premotor cortex, and/or IPL (11,12,15–17,54). A mean residual time series was calculated for each of 52 (26 bilateral) selected ROIs. Pearson correlation coefficients were calculated between the time courses of each pair of selected nodes and Fisher z transformed, generating a 52×52 connectivity matrix for each participant. Network topology was characterized using graph theoretical analyses (55), for which individual connectivity matrices remained weighted, signed, and undirected.

Data-Driven Social Cognitive Network Detection

Social cognitive networks were identified for each participant using the Louvain community detection algorithm for signed networks (56), which divides nodes into modules while maximizing within-module connections and minimizing between-module connections (57). This was done at network densities ranging from the top 20% to 70% of connections (5% intervals). Consensus clustering was then performed to generate individualized network partitions (58), and the process was repeated to produce a group-level consensus partition based on the most frequently assigned module across all consensus partitions (see Supplement).

Graph Metrics

Unthresholded connectivity matrices were split into positive and negative matrices for each participant to calculate graph metrics for each connection type. Graph metrics were then calculated at densities ranging from the top 20% to 50% of connections (5% intervals). A restricted range was used in comparison with that used for consensus clustering given that network density is inherently reduced by separating positive and negative connection

weights, with 50% being the maximum negative matrix density. For the networks identified via consensus clustering, positive and negative within-network connectivity strength (mean sum of connection weights between nodes within each network) and between-network connectivity strength (mean sum of connection weights between nodes in one network and nodes in another network) were calculated (59). Nodal within- and between-network connectivity strengths were calculated similarly.

Division of Sample Based on Social Cognitive Performance

Across all participants, good and poor performance subgroups were generated for both lower- and higher-level social cognition, based on median splits of behavioral factor scores. These lower- and higher-level factor scores were estimated for each participant (60) from observed social cognitive scores, based on our previous two-factor model of social cognition across individuals with SSDs and healthy control participants (6). We also tested this two-factor model in the current sample using confirmatory factor analysis, confirming good fit for the data across participants (comparative fit index = .990, root mean square error of approximation = .042) (see Supplement). The lower-level social cognition factor includes the Penn Emotion Recognition Test, Reading the Mind in the Eyes Test, TASIT 3 Lies, and EA task scores, whereas the higher-level factor is composed of TASIT 2 Simple Sarcasm, TASIT 2 Paradoxical Sarcasm, and TASIT 3 Sarcasm [see Oliver *et al.* (6)].

Statistical Analysis

Data were analyzed using RStudio version 1.1.447 (61). Age, scanner, and sex were included as covariates in all analyses. Analyses were conducted at each density to ensure consistency (see Figure S1), and using the mean values across densities. Mean values and corresponding statistics are reported.

Regression Analyses Across Groups.—Regression analyses were run to interrogate dimensional relationships between connectivity strength and social cognitive performance. Separate multiple regressions were conducted for lower- and higher-level social cognition factor scores, including positive and negative within- and between-network connectivity strengths as predictors and false discovery rate (FDR) correction for multiple comparisons. Age, scanner, and sex were also included as nuisance variables in both models.

Group-Based Comparisons.—Group-based comparisons were used to examine whether connectivity profiles differ in poor versus good lower- and higher-level social cognitive performers and diagnostic groups. Connection type (positive or negative) by network (motor resonance, affect sharing, or mentalizing) analyses of covariance (ANCOVAs) were run for each group comparison (poor vs. good lower-level social cognition; poor vs. good higher-level social cognition; SSDs vs. control) for within- and between-network connectivity strengths. Follow-up pairwise comparisons of estimated marginal means were conducted to interpret significant effects, including Greenhouse–Geisser correction for violations of sphericity where appropriate and FDR correction for multiple comparisons. Nodal within- and between-network connectivity strengths were also compared between groups using *t* tests in the braingraph package (62) for positive and negative connections, including FDR correction for multiple comparisons.

Subanalyses on Prisma Scanners.—Regression analyses and group-based within- and between-network ANCOVAs were also conducted on a subsample of the data collected on Prisma scanners only ($n = 85$) to minimize potential scanner effects.

RESULTS

Participant demographic and clinical characteristics, as well as social cognitive factor scores, are presented in Table 1 (see Tables S1 and S2 for characteristics by performance-based groups).

Data-Driven Social Cognitive Network Detection

Across participants, community detection and consensus clustering revealed three data-driven networks. These networks aligned with a motor resonance network, including the inferior frontal gyrus into premotor cortex, supplementary motor area, IPL, and pSTS; an affect sharing network, including the anterior insula, ACC, and regions of the IPL; and a mentalizing network, including the medial prefrontal cortex, ACC, temporoparietal junction, pSTS, and precuneus (Figure 1) (1). In addition, the same community detection procedure consistently identified three highly similar networks when run separately for good and poor lower- and higher-level social cognition groups, controls alone, and SSDs alone ($\kappa = 0.74$, $p < .0001$).

Network Connectivity

See Table 2 for the group-based main effect and interaction statistics described below, and see the Supplement for sample-wide effect details. See Figure S2 for connectivity strength distributions by groups.

Regression Analyses Across Groups.—Regression analyses including positive and negative within- and between-network connectivity strengths revealed that increased motor resonance–affect sharing negative connectivity, or segregation, was significantly associated with both greater lower-level ($\beta = 0.29$, $p = .0034$, $R^2 = 0.198$) and higher-level ($\beta = 0.27$, $p = .0094$, $R^2 = 0.193$) social cognition factor scores (Figure 2).

Lower-Level Social Cognitive Performance Groups.—Comparison of within-network connectivity in poor versus good lower-level social cognitive performers revealed a significant main effect of performance group, characterized by poor performers showing greater overall within-network connectivity (across connection types) than good performers ($t_{273} = 2.07$, $p = .039$, $d = 0.04$) (Table 2 and Figure 3). However, there was also a significant connection type \times group interaction. Follow-up comparisons with FDR correction demonstrated that poor performers showed greater positive within-network connectivity across all networks than good performers ($t_{525} = 3.10$, $p = .002$, $d = 0.16$) but showed no difference in negative within-network connectivity ($t_{525} = 0.489$, $p > .10$, $d = -0.11$). There were no significant network \times group or network \times connection type \times group interactions.

The ANCOVA comparing between-network connectivity in poor versus good lower-level social cognitive performers also showed a significant connection type \times group interaction. This was driven by reduced between-network negative connectivity or segregation (t_{428}

$= -2.03, p = .043, d = -0.17$) and nonsignificantly greater between-network positive connectivity ($t_{428} = 1.79, p = .074, d = 0.13$) in poor versus good performers. There were no significant effects of performance group, network \times group, or network \times connection type \times group.

Higher-Level Social Cognitive Performance Groups.—The ANCOVA comparing within-network connectivity in poor versus good higher-level social cognitive performance groups revealed a significant network \times connection type \times group interaction (Table 2 and Figure 4). Follow-up comparisons, including FDR correction, showed that this was driven by greater positive connectivity in the mentalizing network ($t_{1433} = 3.09, p = .002, d = 0.32$) and affect sharing network ($t_{1433} = 2.27, p = .024, d = 0.16$) in poor versus good performers but showed no between-group difference in motor resonance positive within-network connectivity ($t_{1433} = -0.691, p > .10, d = 20.09$). Poor performers also demonstrated greater positive connectivity in the mentalizing network than in the motor resonance network ($t_{1055} = 3.54, p = .0004, d = 0.25$), but within-network positive connectivity in these two networks did not differ significantly in good performers ($t_{1055} = -0.635, p > .10, d = -0.14$). There were no significant effects of performance group, network \times group, or connection type \times group.

Comparison of between-network connectivity in poor versus good higher-level social cognitive performers also showed a significant network \times connection type \times group interaction. This was characterized by greater positive ($t_{1129} = 2.02, p = .044, d = 0.24$) and lower negative ($t_{1129} = -2.12, p = .034, d = -0.35$) motor resonance–affect sharing connectivity as well as nonsignificantly lower positive mentalizing–motor resonance connectivity ($t_{1129} = -1.91, p = .057, d = -0.15$) in poor versus good performers. Poor performers also showed greater positive connectivity between the motor resonance network and the affect sharing network than the mentalizing network ($t_{846} = 5.33, p < .0001, d = 0.46$), whereas these between-network positive connectivity values did not differ significantly in good performers ($t_{846} = 0.84, p < .10, d = 0.09$). There were no significant effects of group, network \times group, or connection-type \times group.

Diagnostic Groups.—In contrast to the social cognitive performance–based group comparisons, there were no significant diagnostic group effects or interactions for within- or between-network connectivity (Table 2 and Figure 5).

Subanalyses on Prisma Scanners

The same ANCOVA analyses in the Prisma subsample revealed similar effects for the lower-level social cognition, higher-level social cognition, and diagnostic group comparisons (see Table S3).

Nodal Connectivity

See Table S4 for nodal within- and between-network connectivity results.

DISCUSSION

In a large sample of people with SSDs and healthy control participants, we interrogated within- and between-network functional connectivity of three data-driven social cognitive networks using graph theory during the EA task, by lower- and higher-level social cognitive performance, and by diagnosis. For both lower- and higher-level social cognition, motor resonance–affect sharing negative connectivity was positively associated with social cognitive performance. Social cognitive performance–based group comparisons similarly demonstrated reduced between-network negative connectivity, and greater within-network positive connectivity in poor versus good performers. Taken together, these results suggest that network segregation may be particularly important for optimal social cognitive performance. Functional connectivity differences were associated with social cognitive performance but not with diagnostic group.

Although evidence suggests that social cognition is a multidimensional construct involving dissociable neural regions (7–9), the data-driven identification of three social cognitive networks aligning with motor resonance, affect sharing, and mentalizing provides unique evidence for the distinction of these networks during social cognitive processing. Examining connectivity within and between these networks, motor resonance–affect sharing negative connectivity was a significant dimensional predictor of both lower- and higher-level social cognitive performance across participants. Given that the EA task involves detecting how others are feeling but does not necessarily require emotional empathic responding (35), functional segregation of the motor resonance and affect sharing networks may facilitate more efficient task performance. Indeed, dynamic causal modeling has shown that mentalizing activity can be inhibited by emotional resonance in emotional situations (63). This may suggest that poorer performers use different neurocognitive strategies during the EA task, with mentalizing and motor resonance representing more efficient strategies than affect sharing. This finding also supports the suggestion that the brain is organized into anticorrelated functional networks that may subservise opposing representations or goals (64,65). Furthermore, loss of resting-state network segregation has been linked to psychopathological dimensions in a large sample of healthy youths (34).

The social cognition group comparisons provided further support for these dimensional findings and additional insight into social cognitive network connectivity differences between poor and good social cognitive performers rather than cases versus controls, which may have clinical utility for targeting these deficits. For lower-level social cognition, good versus poor performers showed greater anticorrelation between networks, which coincides with our regression results and may reflect increased functional segregation of these networks and efficient network use, as mentioned. However, this was observed across networks rather than being network specific. Such network-wide effects may have been less discernible in our regression analyses due to the inclusion of network-specific predictors in the models and could reflect the reduced complexity of lower-level abilities, which may more broadly engage these networks. In addition, good versus poor lower-level social cognitive performers showed reduced within- and between-network positive connectivity across networks. This increased widespread positive connectivity could be compensatory in poorer performers, reflecting heightened synchronized activation in regions

extending beyond those that may be most task relevant (66–68). Accordingly, more extensive activation of the mentalizing and motor resonance networks has been seen during emotional imitation in poorer social cognitive performers across individuals with SSDs and healthy control participants (29,69). Widespread cortical–cortical connectivity states in schizophrenia (70) and resting-state hyperconnectivity in autism spectrum disorder (71) have also been associated with greater social impairments. However, more work is needed to determine whether such hyperconnectivity may be driven by broader neural recruitment to perform the same neurocognitive process or by qualitatively different processes.

The results from our dimensional analyses also directly align with those from the higher-level social cognition group comparisons, with good versus poor performers showing greater motor resonance–affect sharing negative connectivity. Additional higher-level social cognition group-based findings support the suggestion that better social cognitive performers may exhibit network efficiency during the EA task, including reduced affect sharing network involvement. Specifically, increased positive connectivity within the affect sharing and mentalizing networks, and between the motor resonance and affect sharing networks, was seen in poor versus good higher-level social cognitive performers. Aligning with this, greater activation during the EA task in affect sharing regions has been associated with lower empathic accuracy in adolescents (37). Increased affect sharing network positive connectivity may be compensatory or may reflect greater emotional resonance (72). Similarly, hyperconnectivity between mentalizing regions, using resting-state and dynamic connectivity during naturalistic fearful clips, has been correlated with greater symptom severity and lower theory of mind performance in SSDs (22,25). Greater positive mentalizing connectivity may be driven by overcompensation in poorer mentalizers or hypermentalizing (overattribution of intentionality), which has been posited and demonstrated in schizophrenia (1,73,74). Greater affect sharing network connectivity and reduced motor resonance–affect sharing functional segregation in worse performers, coinciding with our dimensional results, further emphasizes the importance of differential engagement of these networks during the EA task, and in network segregation more generally, for optimal social cognitive performance.

Notably, diagnostic groups did not appear to differ significantly in social cognitive network connectivity. The inclusion of a large sample of individuals with SSDs likely better captures the range and variability of social abilities in this population (Table 1) compared with more typical case-control studies. This aligns with dimensional work emphasizing the importance of shared patterns of neural structure (31,33) and function (29,30,34) with regard to outcome measures of interest and targeted treatment development. Identifying similar networks across people with SSDs and healthy control participants and connectivity differences, based on social cognitive performance, provides further justification for dimensional approaches within the Research Domain Criteria framework and could apply to other disorders with social cognitive impairments.

Social cognitive networks or seeds are often defined based on meta-analytic results of task-based activation, which might not reflect how social cognitive regions interact during naturalistic social processing. In the current paper, we uniquely defined networks using community detection across broadly selected cortical social cognitive ROIs. Interestingly,

the data-driven parcellation of regions into motor resonance (11,12), affect sharing or emotional empathy (15,54), and mentalizing (16,17) networks largely aligned with meta-analyses of fMRI studies. Notably, despite the benefits of examining online social processing, the chosen task could influence the generalizability of our findings. Participants provide valence ratings during the task, and it is possible that empathic accuracy for different emotion types may have different neural or behavioral correlates (75). However, the EA task involves dynamic, relatively naturalistic social cognitive processing, increasing its ecological validity, and the use of background connectivity analyses should reduce the impact of stimulus-specific responses. Similarly, although we have provided evidence for the construct validity of the lower- and higher-level social cognitive factor scores (6), the social cognitive tasks contributing to these scores have exhibited varying psychometric properties (76), which could influence performance-based group membership. In addition to harmonizing acquisition parameters across scanners, weekly phantom scans ensured sequence stability over time, and standardized operating procedures minimized inter-site variance. Our group has also provided objective evidence for intersite stability (77–79). Furthermore, demonstrating similar between-group findings in our Prisma subsample suggests that scanner effects did not drive these results. Lastly, although we did not control for medication or duration of illness, the finding that connectivity patterns differed by social cognitive performance-based groups, but not by diagnosis, suggests that these variables were likely not driving our effects.

To our knowledge, this study marks the first use of graph theory to detect social cognitive networks and interrogate within- and between-network connectivity during online social processing in SSDs. Furthermore, our large sample allowed for dimensional and performance-based analyses versus a categorical diagnostic approach, revealing functional connectivity differences based on social cognitive performance rather than diagnosis. Thus, the neural circuitry of social cognitive performance may exist dimensionally, which would have important prognostic and therapeutic implications because subgroups with overlapping brain–behavior relationships may be more homogeneous in etiology and treatment response. Our findings suggest that better social cognitive performers exhibit greater segregation between social cognitive networks, whereas worse social cognitive performers may compensate via hyperconnectivity within and between networks. The validation of such brain–behavior relationships could serve to guide targeted treatment development for those exhibiting particular social cognitive deficits.

Supplementary Material

Refer to Web version on PubMed Central for supplementary material.

ACKNOWLEDGMENTS AND DISCLOSURES

This work was supported by the National Institute of Mental Health (Grant Nos. 1/3R01MH102324-01 [to ANV], 2/3R01MH102313-01 [to AKM], and 3/3R01MH102318-01 [to RWB]).

We thank all participants for their contribution to this work and the research staff who performed data collection and management.

Results from the manuscript were presented in part at the 74th Annual Meeting of the Society of Biological Psychiatry, Chicago, IL (May 2019), the Annual Meeting of the Social & Affective Neuroscience Society, Miami, FL (May 2019), and the Congress of the Schizophrenia International Research Society, Orlando, FL (April 2019).

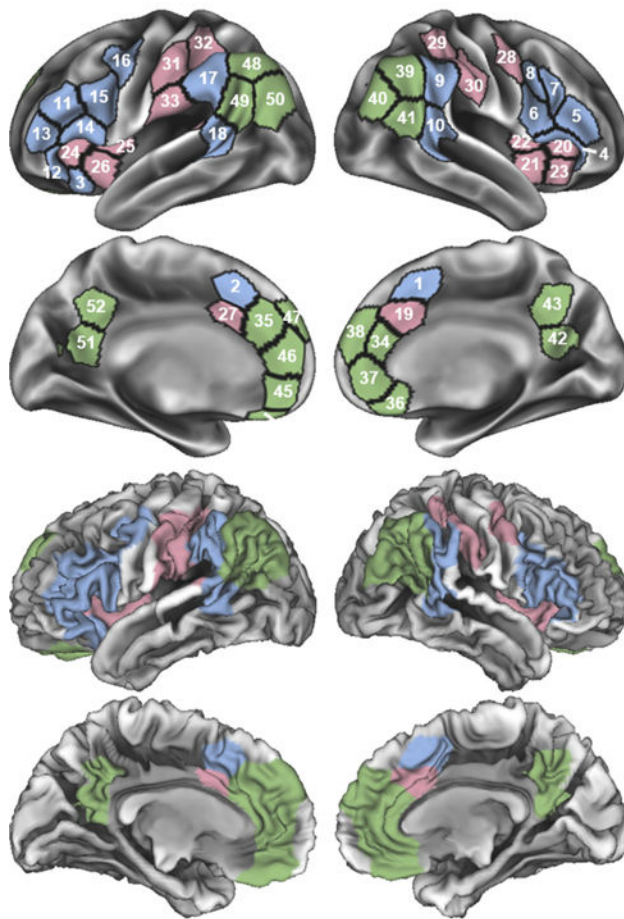
REFERENCES

1. Green MF, Horan WP, Lee J (2015): Social cognition in schizophrenia. *Nat Rev Neurosci* 16:620–631. [PubMed: 26373471]
2. Savla GN, Vella L, Armstrong CC, Penn DL, Twamley EW (2013): Deficits in domains of social cognition in schizophrenia: A meta-analysis of the empirical evidence. *Schizophr Bull* 39:979–992. [PubMed: 22949733]
3. Couture SM, Penn DL, Roberts DL (2006): The functional significance of social cognition in schizophrenia: A review. *Schizophr Bull* 32(suppl 1):S44–S63. [PubMed: 16916889]
4. Green MF, Penn DL, Bentall R, Carpenter WT, Gaebel W, Gur RC, et al. (2008): Social cognition in schizophrenia: An NIMH workshop on definitions, assessment, and research opportunities. *Schizophr Bull* 34:1211–1220. [PubMed: 18184635]
5. Fett AK, Viechtbauer W, Dominguez MD, Penn DL, van Os J, Krabbendam L (2011): The relationship between neurocognition and social cognition with functional outcomes in schizophrenia: A meta-analysis. *Neurosci Biobehav Rev* 35:573–588. [PubMed: 20620163]
6. Oliver LD, Haltigan JD, Gold JM, Foussias G, DeRosse P, Buchanan RW, et al. (2019): Lower- and higher-level social cognitive factors across individuals with schizophrenia spectrum disorders and healthy controls: Relationship with neurocognition and functional outcome. *Schizophr Bull* 45:629–638. [PubMed: 30107517]
7. Shamay-Tsoory SG (2011): The neural bases for empathy. *Neuroscientist* 17:18–24. [PubMed: 21071616]
8. Ochsner KN (2008): The social-emotional processing stream: Five core constructs and their translational potential for schizophrenia and beyond. *Biol Psychiatry* 64:48–61. [PubMed: 18549876]
9. Alcalá-López D, Vogeley K, Binkofski F, Bzdok D (2019): Building blocks of social cognition: Mirror, mentalize, share? *Cortex* 118:4–18. [PubMed: 29903609]
10. Iacoboni M (2009): Imitation, empathy, and mirror neurons. *Annu Rev Psychol* 60:653–670. [PubMed: 18793090]
11. Molenberghs P, Cunnington R, Mattingley JB (2012): Brain regions with mirror properties: A meta-analysis of 125 human fMRI studies. *Neurosci Biobehav Rev* 36:341–349. [PubMed: 21782846]
12. Caspers S, Zilles K, Laird AR, Eickhoff SB (2010): ALE meta-analysis of action observation and imitation in the human brain. *NeuroImage* 50:1148–1167. [PubMed: 20056149]
13. Carr L, Iacoboni M, Dubeau MC, Mazziotta JC, Lenzi GL (2003): Neural mechanisms of empathy in humans: A relay from neural systems for imitation to limbic areas. *Proc Natl Acad Sci U S A* 100:5497–5502. [PubMed: 12682281]
14. Oliver LD, Vieira JB, Neufeld RWJ, Dziobek I, Mitchell DGV (2018): Greater involvement of action simulation mechanisms in emotional versus cognitive empathy. *Soc Cogn Affect Neurosci* 13:367–380. [PubMed: 29462481]
15. Bzdok D, Schilbach L, Vogeley K, Schneider K, Laird AR, Langner R, et al. (2012): Parsing the neural correlates of moral cognition: ALE meta-analysis on morality, theory of mind, and empathy. *Brain Struct Funct* 217:783–796. [PubMed: 22270812]
16. Carrington SJ, Bailey AJ (2009): Are there theory of mind regions in the brain? A review of the neuroimaging literature. *Hum Brain Mapp* 30:2313–2335. [PubMed: 19034900]
17. Schurz M, Radua J, Aichhorn M, Richlan F, Perner J (2014): Fractionating theory of mind: A meta-analysis of functional brain imaging studies. *Neurosci Biobehav Rev* 42:9–34. [PubMed: 24486722]
18. Kronbichler L, Tschernegg M, Martin AI, Schurz M, Kronbichler M (2017): Abnormal brain activation during theory of mind tasks in schizophrenia: A meta-analysis. *Schizophr Bull* 43:1240–1250. [PubMed: 28575475]

19. Taylor SF, Kang J, Brege IS, Tso IF, Hosanagar A, Johnson TD (2012): Meta-analysis of functional neuroimaging studies of emotion perception and experience in schizophrenia. *Biol Psychiatry* 71:136–145. [PubMed: 21993193]
20. Erdeniz B, Serin E, Ibadi Y, Tas C (2017): Decreased functional connectivity in schizophrenia: The relationship between social functioning, social cognition and graph theoretical network measures. *Psychiatry Res Neuroimaging* 270:22–31. [PubMed: 29017061]
21. Mothersill O, Tangney N, Morris DW, McCarthy H, Frodl T, Gill M, et al. (2017): Further evidence of alerted default network connectivity and association with theory of mind ability in schizophrenia. *Schizophr Res* 184:52–58. [PubMed: 27913157]
22. Abram SV, Wisner KM, Fox JM, Barch DM, Wang L, Csernansky JG, et al. (2017): Fronto-temporal connectivity predicts cognitive empathy deficits and experiential negative symptoms in schizophrenia. *Hum Brain Mapp* 38:1111–1124. [PubMed: 27774734]
23. Choe E, Lee TY, Kim M, Hur JW, Yoon YB, Cho KK, et al. (2018): Aberrant within- and between-network connectivity of the mirror neuron system network and the mentalizing network in first episode psychosis. *Schizophr Res* 199:243–249. [PubMed: 29599093]
24. Schilbach L, Derntl B, Aleman A, Caspers S, Clos M, Diederer KM, et al. (2016): Differential patterns of dysconnectivity in mirror neuron and mentalizing networks in schizophrenia. *Schizophr Bull* 42:1135–1148. [PubMed: 26940699]
25. Hendler T, Raz G, Shimrit S, Jacob Y, Lin T, Roseman L, et al. (2018): Social affective context reveals altered network dynamics in schizophrenia patients. *Transl Psychiatry* 8:29. [PubMed: 29382814]
26. Martin AK, Dzafic I, Robinson GA, Reutens D, Mowry B (2016): Mentalizing in schizophrenia: A multivariate functional MRI study. *Neuropsychologia* 93:158–166. [PubMed: 27793657]
27. Mier D, Eisenacher S, Rausch F, Englisch S, Gerchen MF, Zamoscik V, et al. (2017): Aberrant activity and connectivity of the posterior superior temporal sulcus during social cognition in schizophrenia. *Eur Arch Psychiatry Clin Neurosci* 267:597–610. [PubMed: 27770284]
28. Mukherjee P, Whalley HC, McKirdy JW, Sprengelmeyer R, Young AW, McIntosh AM, et al. (2014): Altered amygdala connectivity within the social brain in schizophrenia. *Schizophr Bull* 40:152–160. [PubMed: 23851067]
29. Hawco C, Buchanan RW, Calarco N, Mulsant BH, Viviano JD, Dickie EW, et al. (2019): Separable and replicable neural strategies during social brain function in people with and without severe mental illness. *Am J Psychiatry* 176:521–530. [PubMed: 30606045]
30. Easson AK, Fatima Z, McIntosh AR (2019): Functional connectivity-based subtypes of individuals with and without autism spectrum disorder. *Netw Neurosci* 3:344–362. [PubMed: 30793086]
31. Stefanik L, Erdman L, Ameis SH, Foussias G, Mulsant BH, Behdinan T, et al. (2018): Brain-behavior participant similarity networks among youth and emerging adults with schizophrenia spectrum, autism spectrum, or bipolar disorder and matched controls. *Neuropsychopharmacology* 43:1180–1188. [PubMed: 29105664]
32. Cuthbert BN (2014): The RDoC framework: Facilitating transition from ICD/DSM to dimensional approaches that integrate neuroscience and psychopathology. *World Psychiatry* 13:28–35. [PubMed: 24497240]
33. Rodrigue AL, McDowell JE, Tandon N, Keshavan MS, Tamminga CA, Pearlson GD, et al. (2018): Multivariate relationships between cognition and brain anatomy across the psychosis spectrum. *Biol Psychiatry Cogn Neurosci Neuroimaging* 3:992–1002. [PubMed: 29759822]
34. Xia CH, Ma Z, Ciric R, Gu S, Betzel RF, Kaczkurkin AN, et al. (2018): Linked dimensions of psychopathology and connectivity in functional brain networks. *Nat Commun* 9:3003. [PubMed: 30068943]
35. Zaki J, Weber J, Bolger N, Ochsner K (2009): The neural bases of empathic accuracy. *Proc Natl Acad Sci U S A* 106:11382–11387.
36. Harvey PO, Zaki J, Lee J, Ochsner K, Green MF (2013): Neural substrates of empathic accuracy in people with schizophrenia. *Schizophr Bull* 39:617–628. [PubMed: 22451493]
37. Kral TRA, Solis E, Mumford JA, Schuyler BS, Flook L, Rifken K, et al. (2017): Neural correlates of empathic accuracy in adolescence. *Soc Cogn Affect Neurosci* 12:1701–1710. [PubMed: 28981837]

38. Kern RS, Penn DL, Lee J, Horan WP, Reise SP, Ochsner KN, et al. (2013): Adapting social neuroscience measures for schizophrenia clinical trials, part 2: Trolling the depths of psychometric properties. *Schizophr Bull* 39:1201–1210. [PubMed: 24072805]
39. Olbert CM, Penn DL, Kern RS, Lee J, Horan WP, Reise SP, et al. (2013): Adapting social neuroscience measures for schizophrenia clinical trials, part 3: Fathoming external validity. *Schizophr Bull* 39:1211–1218. [PubMed: 24072806]
40. Sonkusare S, Breakspear M, Guo C (2019): Naturalistic stimuli in neuroscience: Critically acclaimed. *Trends Cogn Sci* 23:699–714. [PubMed: 31257145]
41. Bartels A, Zeki S (2004): Functional brain mapping during free viewing of natural scenes. *Hum Brain Mapp* 21:75–85. [PubMed: 14755595]
42. Al-Aidroos N, Said CP, Turk-Browne NB (2012): Top-down attention switches coupling between low-level and high-level areas of human visual cortex. *Proc Natl Acad Sci U S A* 109:14675–14680.
43. Norman-Haignere SV, McCarthy G, Chun MM, Turk-Browne NB (2012): Category-selective background connectivity in ventral visual cortex. *Cereb Cortex* 22:391–402. [PubMed: 21670097]
44. Gratton C, Laumann TO, Gordon EM, Adeyemo B, Petersen SE (2016): Evidence for two independent factors that modify brain networks to meet task goals. *Cell Rep* 17:1276–1288. [PubMed: 27783943]
45. Kohler CG, Bilker W, Hagendoorn M, Gur RE, Gur RC (2000): Emotion recognition deficit in schizophrenia: Association with symptomatology and cognition. *Biol Psychiatry* 48:127–136. [PubMed: 10903409]
46. Baron-Cohen S, Wheelwright S, Hill J, Raste Y, Plumb I (2001): The “Reading the Mind in the Eyes” Test revised version: A study with normal adults, and adults with Asperger syndrome or high-functioning autism. *J Child Psychol Psychiatry* 42:241–251. [PubMed: 11280420]
47. McDonald S, Flanagan S, Rollins J (2011): *The Awareness of Social Inference Test–Revised (TASIT-R)*. Sydney, Australia: Pearson Assessment.
48. Viviano JD, Buchanan RW, Calarco N, Gold JM, Foussias G, Bhagwat N, et al. (2018): Resting-state connectivity biomarkers of cognitive performance and social function in individuals with schizophrenia spectrum disorder and healthy control subjects. *Biol Psychiatry* 84:665–674. [PubMed: 29779671]
49. Cole MW, Bassett DS, Power JD, Braver TS, Petersen SE (2014): Intrinsic and task-evoked network architectures of the human brain. *Neuron* 83:238–251. [PubMed: 24991964]
50. Satterthwaite TD, Elliott MA, Gerraty RT, Ruparel K, Loughead J, Calkins ME, et al. (2013): An improved framework for confound regression and filtering for control of motion artifact in the pre-processing of resting-state functional connectivity data. *NeuroImage* 64:240–256. [PubMed: 22926292]
51. Muschelli J, Nebel MB, Caffo BS, Barber AD, Pekar JJ, Mostofsky SH (2014): Reduction of motion-related artifacts in resting state fMRI using aCompCor. *NeuroImage* 96:22–35. [PubMed: 24657780]
52. Shen X, Tokoglu F, Papademetris X, Constable RT (2013): Groupwise whole-brain parcellation from resting-state fMRI data for network node identification. *NeuroImage* 82:403–415. [PubMed: 23747961]
53. Finn ES, Shen X, Scheinost D, Rosenberg MD, Huang J, Chun MM, et al. (2015): Functional connectome fingerprinting: Identifying individuals using patterns of brain connectivity. *Nat Neurosci* 18:1664–1671. [PubMed: 26457551]
54. Timmers I, Park AL, Fischer MD, Kronman CA, Heathcote LC, Hernandez JM, et al. (2018): Is empathy for pain unique in its neural correlates? A meta-analysis of neuroimaging studies of empathy. *Front Behav Neurosci* 12:289. [PubMed: 30542272]
55. Bullmore ET, Bassett DS (2011): Brain graphs: Graphical models of the human brain connectome. *Annu Rev Clin Psychol* 7:113–140. [PubMed: 21128784]
56. Rubinov M, Sporns O (2010): Complex network measures of brain connectivity: Uses and interpretations. *NeuroImage* 52:1059–1069. [PubMed: 19819337]
57. Fornito A, Zalesky A, Bullmore ET (2016): *Fundamentals of Brain Network Analysis*. Amsterdam: Elsevier/Academic Press.

58. Lancichinetti A, Fortunato S (2012): Consensus clustering in complex networks. *Sci Rep* 2:336. [PubMed: 22468223]
59. Cohen JR, D'Esposito M (2016): The segregation and integration of distinct brain networks and their relationship to cognition. *J Neurosci* 36:12083–12094. [PubMed: 27903719]
60. Rosseel Y (2012): lavaan: An R package for structural equation modeling. *J Stat Softw* 48:1–36.
61. RStudioTeam (2016): RStudio: Integrated Development for R. Boston: RStudio, Inc.
62. Watson CG (2018): brainGraph: Graph Theory Analysis of Brain MRI Data. R package version 2.2.0. Available at: <https://github.com/cwatson/brainGraph>.
63. Kanske P, Bockler A, Trautwein FM, Parianen Lesemann FH, Singer T (2016): Are strong empathizers better mentalizers? Evidence for independence and interaction between the routes of social cognition. *Soc Cogn Affect Neurosci* 11:1383–1392. [PubMed: 27129794]
64. Fox MD, Snyder AZ, Vincent JL, Corbetta M, Van Essen DC, Raichle ME (2005): The human brain is intrinsically organized into dynamic, anticorrelated functional networks. *Proc Natl Acad Sci U S A* 102:9673–9678. [PubMed: 15976020]
65. Chai XJ, Castanon AN, Ongur D, Whitfield-Gabrieli S (2012): Anticorrelations in resting state networks without global signal regression. *NeuroImage* 59:1420–1428. [PubMed: 21889994]
66. Hillary FG, Roman CA, Venkatesan U, Rajtmajer SM, Bajo R, Castellanos ND (2015): Hyperconnectivity is a fundamental response to neurological disruption. *Neuropsychology* 29:59–75. [PubMed: 24933491]
67. Anticevic A, Hu X, Xiao Y, Hu J, Li F, Bi F, et al. (2015): Early-course unmedicated schizophrenia patients exhibit elevated prefrontal connectivity associated with longitudinal change. *J Neurosci* 35:267–286. [PubMed: 25568120]
68. Fornito A, Zalesky A, Breakspear M (2015): The connectomics of brain disorders. *Nat Rev Neurosci* 16:159–172. [PubMed: 25697159]
69. Hawco C, Kovacevic N, Malhotra AK, Buchanan RW, Viviano JD, Iacoboni M, et al. (2017): Neural activity while imitating emotional faces is related to both lower and higher-level social cognitive performance. *Sci Rep* 7:1244. [PubMed: 28455517]
70. Rabany L, Brocke S, Calhoun VD, Pittman B, Corbera S, Wexler BE, et al. (2019): Dynamic functional connectivity in schizophrenia and autism spectrum disorder: Convergence, divergence and classification. *NeuroImage Clin* 24:101966.
71. Supekar K, Uddin LQ, Khouzam A, Phillips J, Gaillard WD, Kenworthy LE, et al. (2013): Brain hyperconnectivity in children with autism and its links to social deficits. *Cell Rep* 5:738–747. [PubMed: 24210821]
72. Bernhardt BC, Singer T (2012): The neural basis of empathy. *Annu Rev Neurosci* 35:1–23. [PubMed: 22715878]
73. Frith CD (2004): Schizophrenia and theory of mind. *Psychol Med* 34:385–389. [PubMed: 15259823]
74. Ciaramidaro A, Bolte S, Schlitt S, Hainz D, Poustka F, Weber B, et al. (2015): Schizophrenia and autism as contrasting minds: Neural evidence for the hypo-hyper-intentionality hypothesis. *Schizophr Bull* 41:171–179. [PubMed: 25210055]
75. Le BM, Cote S, Stellar J, Impett EA (2020): The distinct effects of empathic accuracy for a romantic partner's appeasement and dominance emotions. *Psychol Sci* 31:607–622. [PubMed: 32422074]
76. Pinkham AE, Harvey PD, Penn DL (2018): Social cognition psychometric evaluation: Results of the final validation study. *Schizophr Bull* 44:737–748. [PubMed: 28981848]
77. Chavez S, Viviano J, Zamyadi M, Kingsley PB, Kochunov P, Strother S, et al. (2018): A novel DTI-QA tool: Automated metric extraction exploiting the sphericity of an agar filled phantom. *Magn Reson imaging* 46:28–39. [PubMed: 29054737]
78. Hawco C, Viviano JD, Chavez S, Dickie EW, Calarco N, Kochunov P, et al. (2018): A longitudinal human phantom reliability study of multicenter T1-weighted, DTI, and resting state fMRI data. *Psychiatry Res Neuroimaging* 282:134–142. [PubMed: 29945740]
79. Kochunov P, Dickie EW, Viviano JD, Turner J, Kingsley PB, Jahanshad N, et al. (2018): Integration of routine QA data into mega-analysis may improve quality and sensitivity of multisite diffusion tensor imaging studies. *Hum Brain Mapp* 39:1015–1023. [PubMed: 29181875]



Label	Region	Label	Region
Motor Resonance Network			
1 R SMA	supplementary motor area	10 R pSTS	posterior superior temporal sulcus
2 L SMA	supplementary motor area	11 L IFG BA45 1	inferior frontal gyrus
3 L AI 1	anterior insula	12 L IFG BA45 2	inferior frontal gyrus
4 R IFG BA44/45	inferior frontal gyrus	13 L IFG BA45 3	inferior frontal gyrus
5 R IFG BA45	inferior frontal gyrus	14 L IFG BA44/45	inferior frontal gyrus
6 R IFG BA44/6 1	inferior frontal gyrus	15 L IFG BA44	inferior frontal gyrus
7 R IFG BA44	inferior frontal gyrus	16 L PMC	premotor cortex
8 R IFG BA44/6 2	inferior frontal gyrus	17 L IPL	inferior parietal lobule
9 R IPL/TPJ 1	inferior parietal lobule/ temporoparietal junction	18 L pSTS/MTG	posterior superior temporal sulcus/mid temporal gyrus
Affect Sharing Network			
19 R dACC 1	dorsal anterior cingulate cortex	27 L mid-ACC	mid anterior cingulate cortex
20 R AI 1	anterior insula	28 R PMC	premotor cortex
21 R AI 2	anterior insula	29 R IPL/IPS	inferior parietal lobule/ intraparietal sulcus
22 R AI 3	anterior insula	30 R SMG	supramarginal gyrus
23 R AI 4	anterior insula	31 L IPL/SMG	inferior parietal lobule/supramarginal gyrus
24 L AI 2	anterior insula	32 L IPS	intraparietal sulcus
25 L AI 3	anterior insula	33 L pSTG/IPL	posterior superior temporal gyrus/inferior parietal lobule
26 L AI 4	anterior insula		
Mentalizing Network			
34 R dACC 2	dorsal anterior cingulate cortex	44 L OFC	orbitofrontal cortex
35 L dACC	dorsal anterior cingulate cortex	45 L mpFC 1	medial prefrontal cortex
36 R vmPFC/ACC	ventromedial prefrontal cortex/ anterior cingulate cortex	46 L mpFC 2	medial prefrontal cortex
37 R mPFC/ACC	medial prefrontal cortex/ anterior cingulate cortex	47 L dmPFC	dorsomedial prefrontal cortex
38 R dmPFC	dorsomedial prefrontal cortex	48 L IPL	inferior parietal lobule
39 R IPL/TPJ 2	inferior parietal lobule/ temporoparietal junction	49 L IPL/STS	inferior parietal lobule/ superior temporal sulcus
40 R pTPJ	posterior temporoparietal junction	50 L pTPJ	posterior temporoparietal junction
41 R IPL/TPJ 3	inferior parietal lobule /temporoparietal junction	51 L Pcun 1	precuneus
42 R Pcun 1	precuneus	52 L Pcun 2	precuneus
43 R Pcun 2	precuneus		

R = right, L = left, BA = Brodmann area

Figure 1. Social cognitive networks identified using community detection and consensus clustering across individuals with schizophrenia spectrum disorders and healthy control participants.

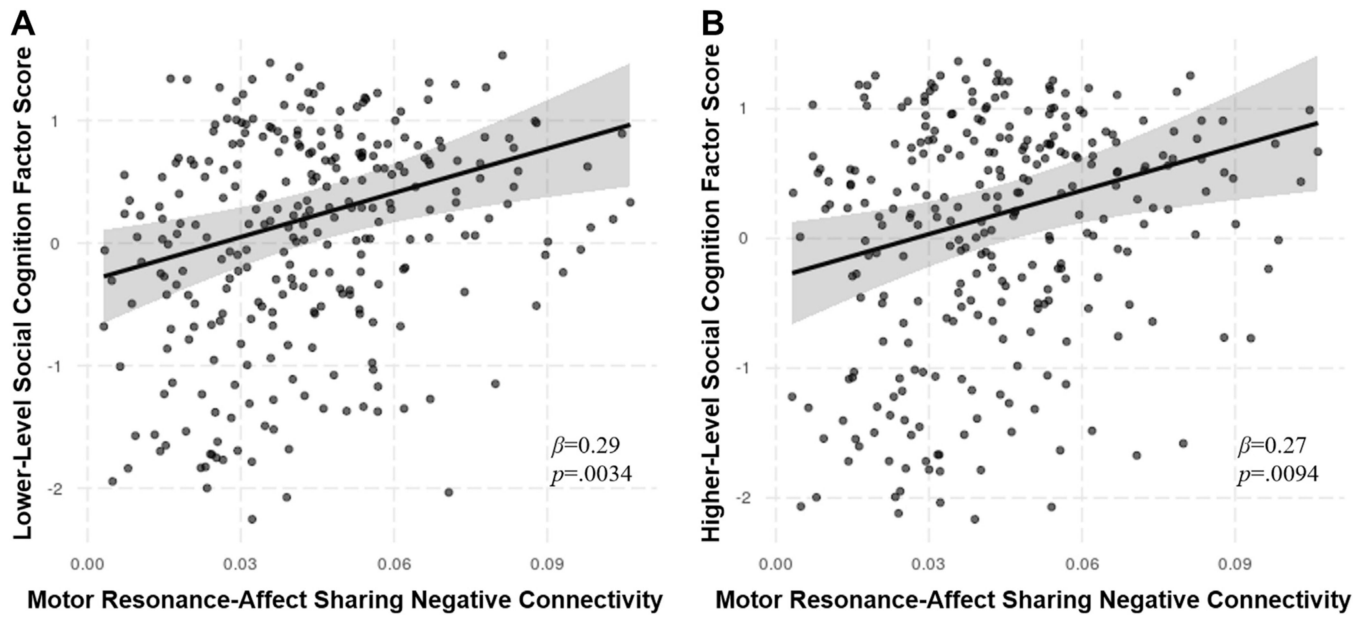


Figure 2. Significant dimensional predictors of lower- and higher-level social cognition factor scores. Plots display the effect of motor resonance–affect sharing negative connectivity on lower-level (**A**) and higher-level (**B**) social cognition factor scores from regression models with 95% confidence intervals.

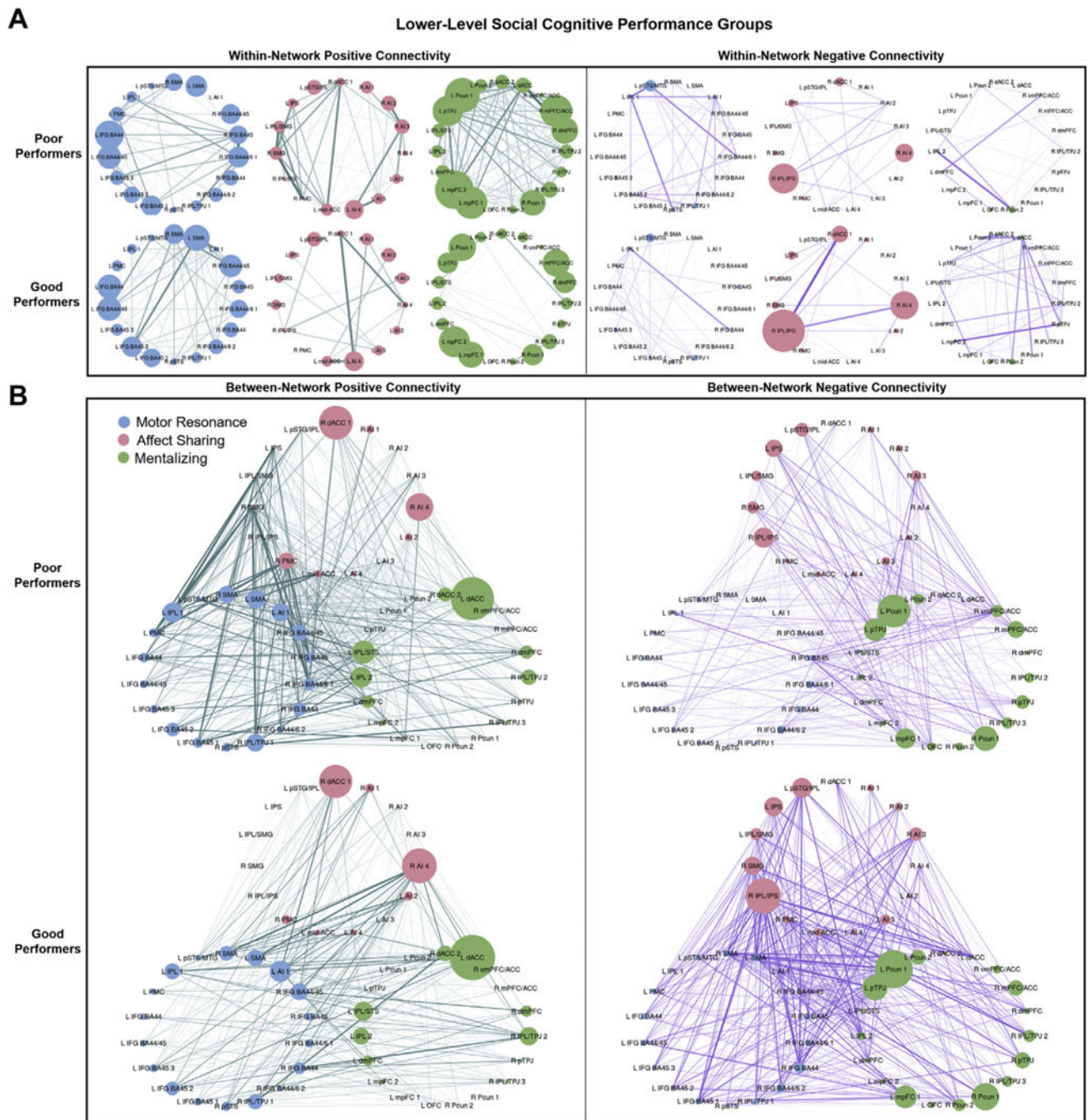


Figure 3. Positive and negative within- and between-network connectivity strengths by lower-level social cognitive performance group. Connectivity strengths for poor and good lower-level social cognitive performance groups are shown. Edge width corresponds to the between-group difference in connection weight. **(A)** Within-network positive (left) and negative (right) connectivity strengths for motor resonance, affect sharing, and mentalizing networks. Node size corresponds to the within-network connectivity strength of the node (sum of within-network connections to the node). **(B)** Between-network positive (left) and negative

(right) connectivity strengths for motor resonance, affect sharing, and mentalizing networks. Node size corresponds to the between-network connectivity strength of the node (sum of between-network connections to the node). See Figure 1 for abbreviations.

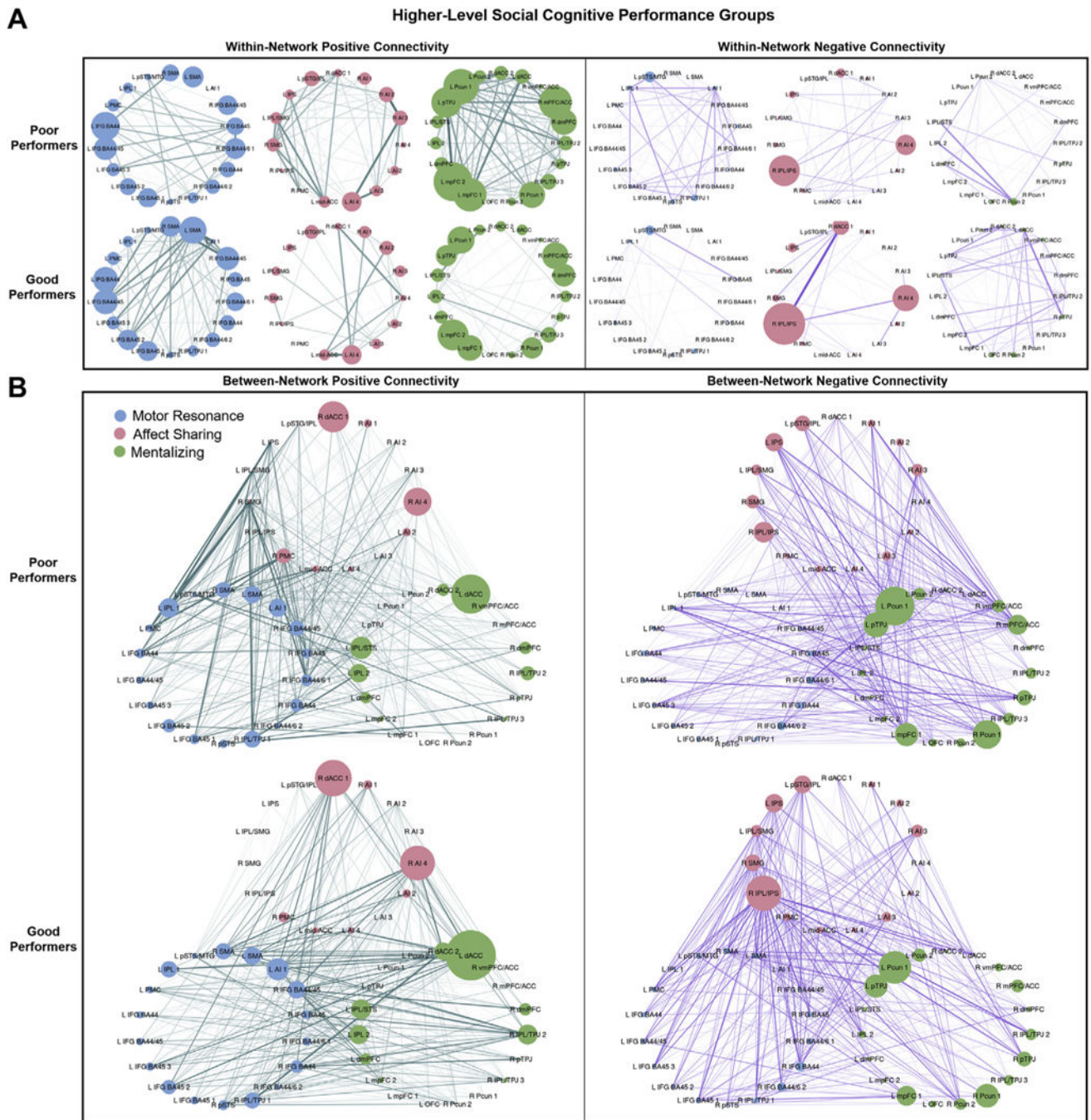


Figure 4. Positive and negative within- and between-network connectivity strengths by higher-level social cognitive performance group. Connectivity strengths for poor and good higher-level social cognitive performance groups are shown. Edge width corresponds to the between-group difference in connection weight. **(A)** Within-network positive (left) and negative (right) connectivity strengths for motor resonance, affect sharing, and mentalizing networks. Node size corresponds to the within-network connectivity strength of the node (sum of within-network connections to the node). **(B)** Between-network positive (left) and negative

(right) connectivity strengths for motor resonance, affect sharing, and mentalizing networks. Node size corresponds to the between-network connectivity strength of the node (sum of between-network connections to the node). See Figure 1 for abbreviations

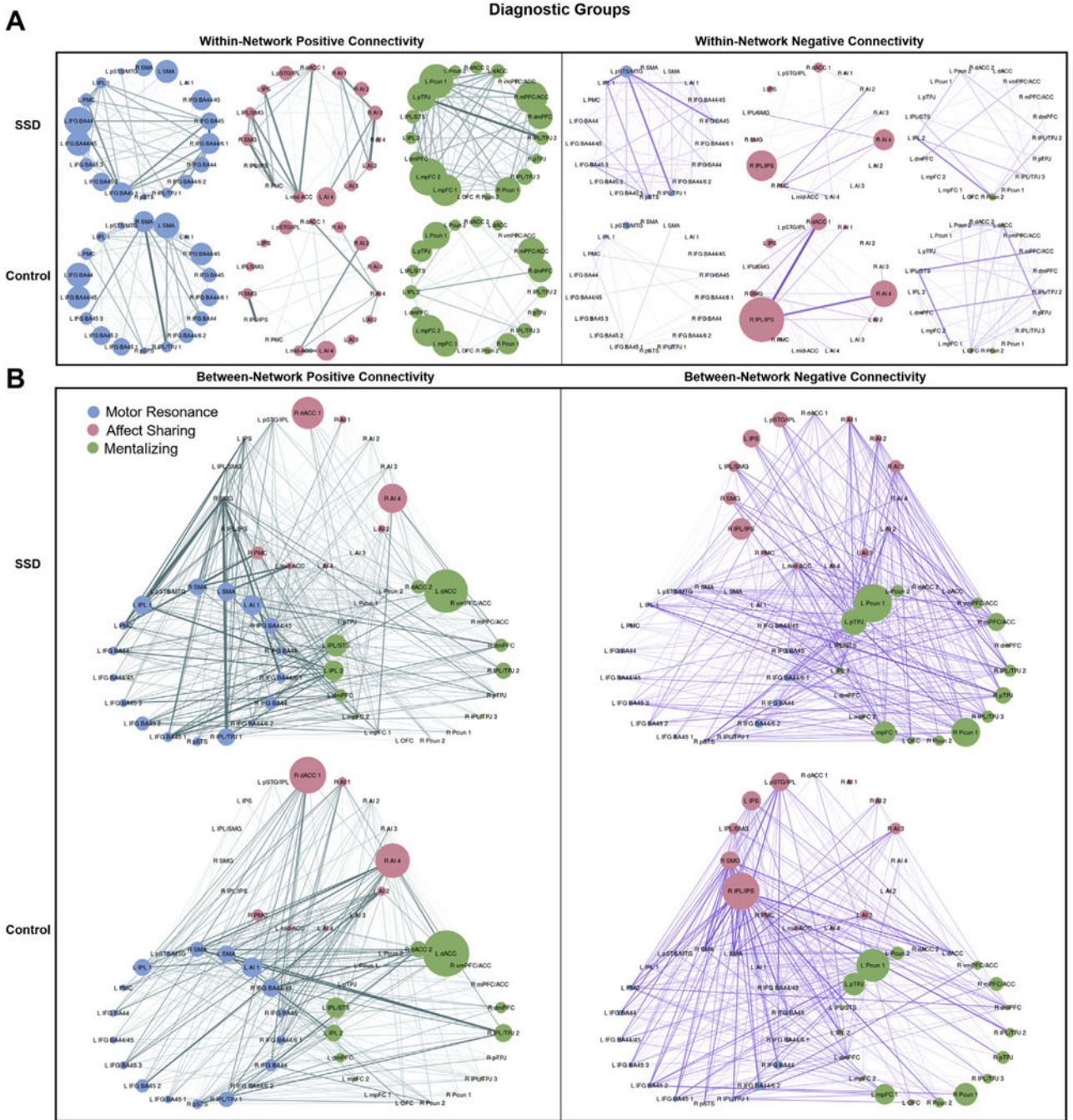


Figure 5. Positive and negative within- and between-network connectivity strengths by diagnostic group. Connectivity strengths for schizophrenia spectrum disorder (SSD) and control groups are shown. Edge width corresponds to the between-group difference in connection weight. **(A)** Within-network positive (left) and negative (right) connectivity strengths for motor resonance, affect sharing, and mentalizing networks. Node size corresponds to the within-network connectivity strength of the node (sum of within-network connections to the node). **(B)** Between-network positive (left) and negative (right) connectivity strengths for motor

resonance, affect sharing, and mentalizing networks. Node size corresponds to the between-network connectivity strength of the node (sum of between-network connections to the node). See Figure 1 for abbreviations

Author Manuscript

Author Manuscript

Author Manuscript

Author Manuscript

Table 1.

Participant Demographic and Clinical Characteristics by Diagnostic Group

	SSD Group (<i>n</i> = 164)	Control Group (<i>n</i> = 117)	<i>P</i>
Performance Groups, Good	54 (32.9%)	86 (73.5%)	<.001
Sex, Male	112 (68.3%)	62 (53.0%)	.013
Age, Years	31.79 (9.54)	32.05 (10.45)	.830
Education, Highest Grade	13.62 (2.17)	15.50 (1.89)	<.001
WTAR, Standard Score	107.38 (14.30)	112.41 (11.58)	.012
BPRS Total	31.57 (8.22)	-	-
SANS Total	24.83 (12.79)	-	-
BSFS Total	136.2 (23.74)	177.17 (20.62)	<.001
Lower-Level Social Cognition Score	-0.28 (0.87)	0.47 (0.67)	<.001
Higher-Level Social Cognition Score	-0.33 (0.89)	0.55 (0.63)	<.001

Values are presented as *n* (%) or mean (SD).

BPRS, Brief Psychiatric Rating Scale; BSFS, Birchwood Social Functioning Scale; SANS, Scale for the Assessment of Negative Symptoms; SSD, schizophrenia spectrum disorder; WTAR, Wechsler Test of Adult Reading.

Table 2. Within- and Between-Network Connectivity Results by Lower-Level Social Cognitive Performance, Higher-Level Social Cognitive Performance, and Diagnostic Groups

	<i>df</i>	<i>F</i>	<i>P</i>	η^2_p
Within-Network Connectivity				
Lower-Level Social Cognitive Performance Group Comparisons				
Network	1.98, 540.75	42.28	<.0001	0.134
Connection type	1, 273	8095.65	<.0001	0.967
Group	1, 273	4.28	.039	0.015
Network × connection type	1.98, 541.74	71.89	<.0001	0.208
Network × group	1.98, 540.75	1.22	.297	0.004
Connection type × group	1, 273	5.36	.021	0.019
Network × connection type × group	1.98, 541.74	1.94	.145	0.007
Higher-Level Social Cognitive Performance Group Comparisons				
Network	1.98, 540.64	42.37	<.0001	0.134
Connection type	1, 273	8015.39	<.0001	0.967
Group	1, 273	2.43	.120	0.009
Network × connection type	1.98, 541.80	72.26	<.0001	0.209
Network × group	1.98, 540.64	1.80	.167	0.007
Connection type × group	1, 273	2.60	.108	0.009
Network × connection type × group	1.98, 541.80	3.38	.035	0.012
Diagnostic Group Comparisons				
Network	1.98, 540.58	42.22	<.0001	0.134
Connection type	1, 273	8005.88	<.0001	0.967
Group	1, 273	2.03	.156	0.007
Network × connection type	1.98, 541.56	71.80	<.0001	0.208
Network × group	1.98, 540.58	0.81	.445	0.003
Connection type × group	1, 273	2.28	.132	0.008
Network × connection type × group	1.98, 541.56	1.61	.202	0.006
Between-Network Connectivity				

	<i>df</i>	<i>F</i>	<i>P</i>	η_p^2
Lower-Level Social Cognitive Performance Group Comparisons				
Network	1.96, 535.36	186.78	<.0001	0.406
Connection type	1, 273	50.89	<.0001	0.157
Group	1, 273	0.06	.806	0.000
Network × connection type	1.69, 461.56	703.40	<.0001	0.720
Network × group	1.96, 535.36	0.30	.737	0.001
Connection type × group	1, 273	4.79	.030	0.017
Network × connection type × group	1.69, 461.56	2.19	.122	0.008
Higher-Level Social Cognitive Performance Group Comparisons				
Network	1.96, 535.70	187.29	<.0001	0.407
Connection type	1, 273	50.03	<.0001	0.155
Group	1, 273	0.19	.664	0.001
Network × Connection type	1.70, 464.46	715.59	<.0001	0.724
Network × group	1.96, 535.70	1.05	.350	0.004
Connection type × group	1, 273	0.08	.781	0.000
Network × connection type × group	1.70, 464.46	6.96	.002	0.025
Diagnostic Group Comparisons				
Network	1.96, 535.39	188.30	<.0001	0.408
Connection type	1, 273	50.15	<.0001	0.155
Group	1, 273	0.75	.386	0.003
Network × connection type	1.69, 460.85	700.13	<.0001	0.719
Network × group	1.96, 535.39	2.53	.082	0.009
Connection type × group	1, 273	0.72	.397	0.003
Network × connection type × group	1.69, 460.85	0.91	.390	0.003